JOURNAL OF VIROLOGY, Dec. 1983, p. 633–640
0022-538X/83/120633-08$02.00/0

Vol. 48, No. 3

Characterization of Replicative Intermediate RNA of Mouse Hepatitis Virus: Presence of Leader RNA Sequences on Nascent Chains

RALPH S. BARIC,* STEPHEN A. STOHLMAN, AND MICHAEL M. C. LAI

Departments of Microbiology and Neurology, University of Southern California School of Medicine, Los Angeles, California 90033

Received 3 June 1983/Accepted 1 September 1983

Mouse hepatitis virus A59 codes for seven mRNAs in infected cells. These mRNAs are transcribed from a minus (−) strand template of genome length and contain a leader RNA at their 5′ ends. To further elucidate the mechanism of coronavirus transcription, we examined the structure of mouse hepatitis virus replicative intermediates (RIs) isolated by 2 M NaCl precipitation and Sepharose 2-B column chromatography. Purified RIs migrated as a single species on agarose gels and sedimented between 12 and 38S on 10 to 25% sucrose gradients. The complexes were readily heat denatured into a heterogeneous population of smaller RNA molecules which probably represent nascent plus (+) strands. RNase A digestion of RIs produced a single replicative form which sedimented between 30 and 32S. These data suggest that the RI is composed of a single genome-sized (−) strand hydrogen bonded to an average of 4 to 6.5 nascent (+) strands. In contrast, a column-purified replicative form was extremely resistant to RNase A digestion and heat denaturation and migrated as a single RNA species on agarose gels and sucrose gradients. Oligonucleotide fingerprinting of an RI revealed the presence of the 5′ leader RNA on the nascent (+) strands. In addition, an average of 6.2 cap structures were present in each RI, which agrees with the average number of nascent (+) strands per RI. These data suggest that the leader RNA is utilized as a primer for mouse hepatitis virus RNA transcription and is not added to mRNA post-transcriptionally.

Mouse hepatitis virus (MHV), a member of the family Coronaviridae, contains a single-stranded and positive-sensed RNA of 5.4×10^6 daltons (15, 25). The genomic RNA sediments at 60S (15, 16) and contains a 5′-terminal cap and a tract of polyadenylic acid [poly(A)] at the 3′ end (16). The 60S genome contains at least seven genes, which encode the three structural proteins (gp180/90, pp60, and gp25) and four or more nonstructural proteins (20, 24). Seven viral mRNAs, ranging from 0.6×10^6 to 5.4×10^6 daltons, are detected on polysomes during MHV infections (13, 18). These intracellular RNAs are polyadenylated and capped and are arranged as a nested set from the 3′ terminus of the genome, so that the sequences of each smaller RNA are conserved at the 3′ end of every larger RNA. Thus, the sequences of each RNA are completely contained within the next larger mRNA species (11).

The complexity of the MHV mRNAs is further demonstrated by several unique structural characteristics. All of these mRNAs share at least five identical nucleotides at the 5′ ends (13). Furthermore, oligonucleotide fingerprint mapping of these RNAs demonstrated that at least two oligonucleotides, 10 and 82, present at the 5′ end of the genome, are conserved at the 5′ end of every mRNA (12, 13). These oligonucleotides are not present elsewhere in the genomic RNA or mRNA (12, 22). Therefore, the sequences at the 5′ ends of the viral mRNAs are not colinear with the sequences in the viral genome. In addition, several unique oligonucleotides which are not present on the genome are present on some mRNAs (11, 13). The most likely interpretation of these data is that a leader RNA is synthesized and joined to the body of mRNA sequences during RNA transcription or by RNA processing post-transcriptionally.

The mechanism of MHV mRNA synthesis has only been partially elucidated. In common with most other plus (+)-stranded RNA viruses, coronaviruses replicate through an intermediate RNA of negative sense (14). Brayton et al. (5) have shown that an RNA-dependent RNA polymerase which is produced immediately after infection is responsible for the synthesis of a

genome-length minus (−)-sensed RNA. Since only a single species of full-length (−)-stranded RNA was detected in infected cells, all of the viral mRNAs have to be transcribed from the same template (P. R. Brayton, S. A. Stohlman, and M. M. C. Lai, submitted for publication). Furthermore, they are probably transcribed independently, since the UV target size of every MHV-specific mRNA is equivalent to its respective physical size (10). This precludes the conventional mechanism of post-transcriptional RNA splicing. Thus, the question is raised as to how leader RNA sequences are joined to the body sequences of each mRNA during transcription or post-transcriptionally.

The replicative-form (RF) RNA in MHV-infected cells, which was obtained by RNase digestion of the double-stranded RNA present in the infected cells, has recently been analyzed. Only one RF RNA species corresponding to the full-length genomic RNA was detected (14). These data suggest that the mechanism of MHV mRNA synthesis is different from that of togaviruses, which also synthesize a subgenomic mRNA (9, 21). To further understand the mechanism of mRNA synthesis, we characterized the replicative-intermediate (RI) RNA in MHV-infected cells. We found that the nascent chains on the RI contained leader sequences, suggesting that the leader RNA is joined to the body sequences of each mRNA during transcription rather than post-transcriptionally. The further implication of this finding on the mechanism of mRNA synthesis is discussed.

MATERIALS AND METHODS

Virus and cells. The A59 strain of MHV, originally provided by C. Bond, University of California, San Diego, was cloned three times on DBT cells before it was used. SAC(−) cells were obtained from Katherine Holmes, Uniformed Services University, Bethesda, Md., and maintained in Dulbecco minimal essential media containing 10% inactivated fetal calf serum. All experiments were performed at 37°C at a multiplicity of infection of 1 to 5.

Radiolabeling and extraction of intracellular RNA. SAC(−) cells in 10 100-mm dishes were infected with strain A59 in the presence of 2 μg of actinomycin D per ml and incubated in phosphate-free medium as previously described (14). Infected cells were labeled with 250 μCi of $^{32}P_i$ (ICN Pharmaceuticals, Inc.) per ml for 0.5 to 1.0 h at 6 h postinfection or with 75 μCi of [^{3}H]uridine (ICN) per ml immediately after infection. In both instances, intracellular RNA was extracted at 7 h postinfection. After the cells were radiolabeled, the cultures were placed on ice and immediately lysed by the addition of 2.5 ml of phenol. The intracellular RNA was purified by vortexing in the presence of 2.5 ml of HTNE buffer (0.1 M NaCl, 1 mM EDTA, 0.1 M Tris-hydrochloride; pH 8.6) containing 1% sodium dodecyl sulfate (SDS). The aqueous phase was extracted again with phenol-chloroform (1:1) and precipitated in 2 to 3 volumes of ethanol at −20°C. Before they were used, the RNA samples were centrifuged at 15,000 × *g* for 15 min and air dried.

Sepharose 2B-CL column chromatography. Intracellular RNA, prepared as described above, was suspended in LSB buffer (1 mM EDTA, 0.01 M Tris-hydrochloride; pH 7.4) and adjusted to 2 M NaCl and 0.05% SDS. Samples were incubated at 4°C for 24 to 30 h and centrifuged at 14,500 rpm for 60 min in a Ti30 rotor (Beckman Instruments, Inc.). The supernatant fraction was diluted with an equal volume of water, and the RNA was precipitated with 2 to 3 volumes of ethanol. This fraction contains RF RNA (14). The 2 M NaCl precipitate was suspended in 2 ml of LSB buffer containing 1% SDS, adjusted to 0.1 M NaCl, and applied to a Sepharose 2B-CL column. This fraction contains MHV mRNAs and RIs. The column was prepared by a modification of the method described by Spector and Baltimore (23). Sepharose 2B-CL was autoclaved, poured into a glass column (98 by 1.5 cm), and equilibrated in NTE buffer (0.1 M NaCl, 1 mM EDTA, 0.01 M Tris-hydrochloride; pH 7.4) containing 1% SDS. After loading, the sample was eluted with the same buffer, fractions (1.3 to 1.4 ml each) were collected, and a portion was counted. Samples of 0.2 ml from each fraction were precipitated with ethanol, suspended in LSB buffer, adjusted to 2× SSC (1× SSC is 0.15 M NaCl and 0.015 M sodium citrate) and digested with 10 μg of RNase A per ml at 37°C for 30 min for the determination of resistance to RNase. Digested samples were spotted on filter papers, and the trichloroacetic acid (TCA)-precipitable material was collected and counted.

Agarose gel electrophoresis. RI-containing fractions were pooled, precipitated, suspended in LSB buffer, and adjusted to 1× RE buffer (50 mM boric acid, 5 mM sodium borate, 10 mM sodium sulfate, 1 mM EDTA) containing 10 to 15% sucrose. Boiled and nonboiled samples were quick-cooled and electrophoresed at 90 V for 5 h in 1% agarose gels as previously described (14). Gels containing [^{32}P]RNA were dried and exposed to Kodak X-R films directly. For [^{3}H]uridine-labeled samples, the gels were impregnated with PPO (2,5-diphenyloxazole)-methanol and dried for fluorography (17).

Sucrose gradient sedimentation. RIs purified by Sepharose 2B-CL column chromatography were analyzed on 10 to 25% sucrose gradients made in NTE buffer containing 0.1% SDS. The material was sedimented at 40,500 rpm for 4.5 h at 20°C in an SW41 rotor (Beckman). Fractions were collected in Eppendorf centrifuge tubes and precipitated with ethanol in the presence of 5 μg of carrier tRNA. RNase-resistant counts in these fractions were determined as described above. For determination of the sedimentation coefficient of MHV RF, RIs were digested with RNase A and sedimented on 10 to 25% sucrose gradients as described above. About 45 fractions were collected, and the TCA-precipitable counts were determined for each fraction.

RNase T_1-resistant oligonucleotide fingerprinting. RIs purified by Sepharose column chromatography and sucrose gradient centrifugation were precipitated with ethanol and suspended in LSB buffer. One-half of the sample was boiled at 100°C for 1 min and quick-cooled. Both denatured and nondenatured samples were digested with 12.5 U of RNase T_1 at 37°C for 1 h. Two-dimensional polyacrylamide gel electrophoresis

was performed as previously described (11). After electrophoresis, the gels were wrapped with cellophane and exposed to Kodak BB-1 film with an intensifying screen at 4°C for 4 to 6 weeks.

Analysis of 5′ cap structures. Column-purified RIs were suspended in LSB buffer and digested with (per ml) 150 U of RNase T_1–5 U of RNase T_2–20 μg of RNase A at pH 4.4 as previously described (16). After digestion, the samples were electrophoresed on DEAE-cellulose paper in pyridine-acetate buffer (pH 3.5) for 5 to 6 h at 1,500 V. The paper was dried and exposed to BB-5 film. Only the area surrounding the predicted cap spot was exposed to an intensifying screen.

RESULTS

Isolation and characterization of MHV RIs. The RNA from the MHV-infected cells was precipitated with 2 M NaCl to separate double-stranded RF from RI and single-stranded RNAs. The supernatant fraction contained RF and small RNAs, which have been previously characterized (14). The precipitate contained single-stranded RNA and partially double-stranded RI. RNAs were separated further by gel filtration chromatography on Sepharose 2B-CL, which has an exclusion limit of 2×10^7 daltons. Since RIs are high-molecular-weight complexes consisting of a single (−) strand hydrogen bonded to two or more nascent (+) strands (1, 23), they will be excluded from the column, whereas the MHV-specific genomic (5.4×10^6 daltons) and subgenomic mRNAs will be included in the column. As shown in Fig. 1A, 2 M NaCl-precipitated intracellular RNAs were separated into two distinct peaks by Sepharose 2B-CL column chromatography. In several experiments, the excluded peak averaged from 38 to 50% resistant to RNase A, indicating that it is partially double stranded and probably represents purified RIs, whereas the second peak was completely sensitive to RNase, suggesting that it contained an MHV genome and mRNAs. In addition, under conditions which preferentially label the growing nascent (+) strands on RIs, i.e., the RNA was pulse-labeled for 15 min at 6 h postinfection, the majority of radioactivity was confined to the excluded peak (data not shown). To demonstrate the purity of RIs in the excluded peak, we rechromatographed a portion of this material through the Sepharose 2B-CL column. As depicted in Fig. 1B, no contaminating MHV mRNAs were detected in the included volume.

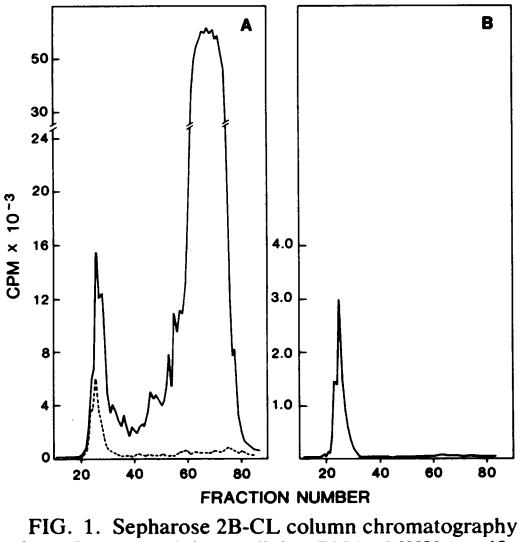

FIG. 1. Sepharose 2B-CL column chromatography of MHV RIs and intracellular RNA. MHV-specific intracellular RNA labeled with [^{3}H]uridine from 1 to 7 h postinfection was precipitated with a high salt concentration and chromatographed on Sepharose 2B-CL agarose beads. A portion of each fraction was analyzed for resistance to RNase. (A) Total 2 M NaCl-precipitated intracellular RNA; (B) repeated chromatography of a portion of the excluded peak. Symbols: ——, TCA-precipitated counts per minute; – – –, RNase-resistant counts per minute.

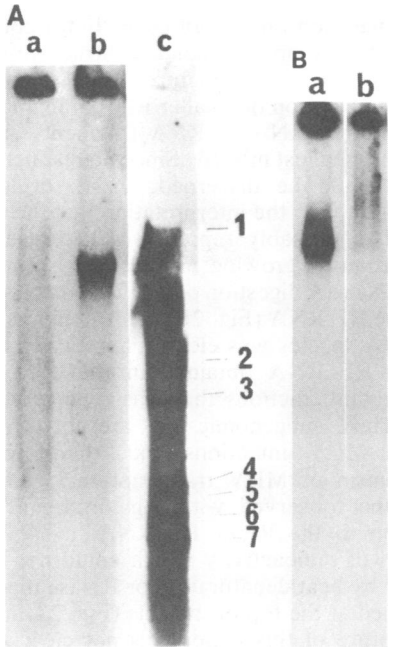

FIG. 2. Agarose gel electrophoresis of MHV RIs. MHV RIs labeled from 1 to 7 h postinfection with $^{32}P_i$ were purified by molecular sieve chromatography and analyzed on 1% agarose gels. RNase digestion of a portion of the RIs was performed as described in the text for analysis of MHV RF. Electrophoresis was at 90 V for 5 h. (A) MHV RIs: a, denatured RI; b, nondenatured RI; c, MHV mRNAs as markers. (B) MHV RF produced from RIs: a, nondenatured RF; b, denatured RF.

Electrophoresis of putative RIs revealed a single RNA species which migrated slightly faster than the genomic RNA on 1% agarose gels (Fig. 2A). The reason for this higher electropho-

retic migration rate is not clear, but it could be due to the complex secondary structure of the RI. RIs were heat denatured into a heterogeneous population of smaller RNAs ranging from the genomic RNA to RNA fragments smaller than the smallest mRNA. Since no distinct RNA bands could be discerned, these results are consistent with the interpretation that the smaller RNAs probably represent a heterogeneous population of growing nascent (+) strands on RIs. RNase A digestion of purified RIs produced a single RF RNA (Fig. 2B). This double-stranded RNA species was electrophoretically identical to RF RNA obtained in the 2 M NaCl supernatant fractions that was reported earlier (14). Thus, subgenomic RFs are not produced during MHV infections and, therefore, the mechanism of MHV transcription is different from that observed with togaviruses (21). In addition to the RI or RF RNA, a significant portion of radioactivity which could not be removed by heat denaturation or RNase digestion remained at the top of the gels (Fig. 2A and B). The nature of this material is not clear, but it could be double-stranded RNA aggregates and possibly some contaminating cellular DNA.

Chromatography of the 2M NaCl supernatant produced a single peak in the excluded volume of the column (data not shown). These fractions were 80 to 90% resistant to RNase A digestion and yielded a single band upon electrophoresis (data not shown). These results are consistent with results reported previously (14) and indicate that these structures are RF RNA.

Biochemical properties of MHV RIs. The number of nascent (+) chains on an RI was determined by the following formula: % resistant to RNase = $2/(2 + n/2)$, where n is the number of growing chains (1). Based on the 38 to 50% resistance to RNase of the MHV RIs, the average number of nascent chains ranged between 4 and 6.5. This number, however, can only be considered tentative, since there are seven mRNA species of different sizes and the abundance of these RNAs varies widely (11, 18). Therefore, the relative number of nascent chains for each mRNA species in the RI structure is not known.

Sedimentation values were also obtained for the column-purified RIs and RF by centrifugation through 10 to 25% sucrose gradients. MHV RIs sedimented as a broad heterogeneous band between 12 and 38S (Fig. 3A). It is noteworthy that the RIs sedimented as a broader peak than did the RF under this condition (Fig. 3B), which supports the data suggesting that RIs are heterogeneous in terms of growing nascent chains. In contrast, the RF obtained either by RNase digestion of the purified RI RNA or directly from the 2 M NaCl-soluble fractions, sedimented as a single RNA species between 30 and 32S, confirming earlier reports of a single RF in MHV infections (Fig. 3B) (14).

Oligonucleotide fingerprinting of MHV RIs. To understand the mechanism of MHV mRNA transcription, we analyzed the sequences contained on the nascent (+) strands of highly purified RIs. The intracellular RNA, obtained from MHV-infected cells labeled with [^{32}P] at 6 h postinfection for 1 h, was separated by Sepharose 2B-CL column chromatography and further purified by sucrose gradient sedimentation. The fractions containing the peak of resistance to RNase (Fig. 3A) were collected and used for RNase T_1-resistant oligonucleotide fingerprinting. Under these conditions, the majority of radioactive label should be confined to (+)-stranded RNA (5; Brayton et al., submitted for publication). These RIs were analyzed by oligonucleotide fingerprinting either with or without heat denaturation before RNase T_1 digestion. The fingerprints of RIs without heat denaturation should represent the sequences present in the single-stranded RNA tails of RIs. As seen in

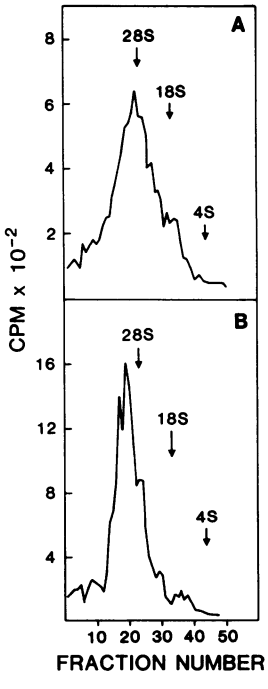

FIG. 3. Sedimentation of MHV RIs or RF on sucrose gradients. MHV-infected cells were labeled with [^{3}H]uridine from 1 to 7 h postinfection and purified as described in the text. MHV RF, derived by RNase digestion of RIs, or RIs were centrifuged through 10 to 25% sucrose gradients in NTE buffer at 40,500 rpm for 4.5 h in an SW41 rotor. Individual fractions were collected and counted as described in the text. (A) MHV RIs; (B) MHV RF.

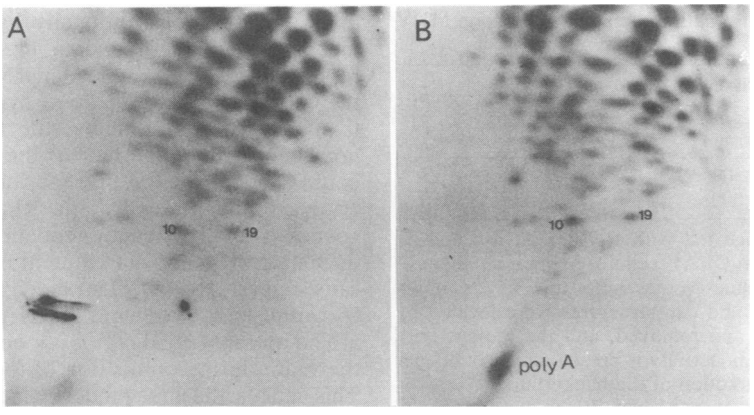

FIG. 4. Oligonucleotide fingerprint mapping of MHV RIs. RIs labeled with $^{32}P_i$ at 6 h postinfection for 30 min were purified by column chromatography and sucrose gradient centrifugation. Only those fractions containing resistance to RNase were collected and digested with RNase T_1. (A) Nondenatured RI; (B) denatured RI.

Fig. 4A, the oligonucleotide fingerprints of undenatured RIs contained essentially all of the large T_1 oligonucleotides present in the genomic RNA, although they were present in different molar ratios. The most prominent oligonucleotides were 10 and 19, which represent the 5′-terminal leader sequences of the genomic and subgenomic mRNAs (12). The abundance of these two oligonucleotides is consistent with the interpretation that these oligonucleotides represent the 5′ ends of all of the nascent chains, since there are, on the average, between 4 and 6.5 nascent chains per RI molecule. The fingerprint of the heat-denatured RI was essentially identical to that of the native RI, except that there was a prominent poly(A) spot in the denatured RI (Fig. 4B). The finding that the poly(A) tract was not detected in the fingerprint of the native RI (Fig. 4A) suggests that the majority of the poly(A) on the nascent (+) strands is annealed to the (−) strand and thus did not enter the first dimension of the fingerprint. The poly(A) tract was released only after heat denaturation. This result suggests that poly(A) is transcribed directly from a polyuridylic acid tract which is present in the (−)-stranded RNA of MHV (J. Leibowitz, personal communication). These data indicate that the 5′ leader sequences are present at the 5′ ends of the nascent mRNA strands during transcription, rather than joined to the body sequences post-transcriptionally, and also suggest that the poly(A) sequences on MHV mRNAs are encoded from the (−) strand.

Analysis of cap structures on MHV RIs. It has been shown that all MHV mRNAs are capped in infected cells (13). It was of interest to determine whether the nascent (+) strands contained 5′ cap structures and to estimate the number that were present on the RIs. Figure 5 clearly shows the presence of the cap structure in nondenatured RI preparations. In addition, a large amount of radioactivity which represented the double-stranded RNA portions (RF) of the RI remained at the origin. To determine the number of cap structures present, we compared the radiolabel incorporated into the cap structures with the total radiolabel in the RF (origin). The latter number should roughly correspond to the molar equivalent of the RI, since only one strand [the (+) strand] was labeled. The results in Table 1 suggest that 6.2 caps are present on each RI. These data are based on the presence of four phosphate groups in each viral mRNA cap structure (13) and on the assumption that 20,000

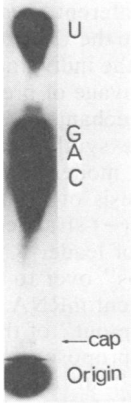

FIG. 5. Analysis of cap structures on MHV RIs. Column-purified RIs prepared as described in the legend to Fig. 4 were digested with RNAses T_1, T_2, and A. Samples were electrophoresed on DEAE-cellulose paper in pyridine-acetate buffer (pH 3.5) for 5 to 6 h at 1,500 V. Only those areas surrounding the predicted cap structures were exposed to an intensifying screen.

TABLE 1. Determination of cap structures on MHV RIs

Expt	Total radioactivity (counts per minute)[a]		Caps per RI[b]
	Origin	Cap	
1	22,500	28	6.2
2	26,000	35	6.7

[a] MHV RIs digested with RNases A, T_1, and T_2 were spotted onto DEAE-cellulose paper and electrophoresed in pyridine-acetate buffer (pH 3.5) as shown in Fig. 5. Origin and cap structures were located by autoradiography and removed, and the radioactivity was counted. Radioactivity is presented as counts per minute after subtraction of the background.

[b] The number of caps per RI is based on the assumption that 20,000 nucleotides are contained in the MHV genome (15).

nucleotides are present in the MHV genome. This number, however, can only be considered tentative, since the counts obtained were relatively low. Nevertheless, the results from these experiments correlate well with our estimates on the number of nascent (+) strands on an RI and indicate that capping occurs during nascent (+) strand synthesis.

DISCUSSION

Previous investigations of the mRNA structure and mechanism of RNA transcription during murine coronavirus replication suggest that a leader RNA is joined to the body sequences of the mRNAs either during or after transcription (12). This process takes place in the cytoplasm of infected cells, since MHV replicates efficiently in enucleated cells (4, 27). This joining process is apparently different from the conventional RNA splicing, since the UV transcriptional mapping suggests that the individual mRNAs are not derived by the cleavage of precursor RNA (10). Several possible mechanisms could be proposed to account for the synthesis of such mRNAs (Fig. 6). In the first model, the RNA polymerase initiates the synthesis of the leader RNA from the 3′ end of the (−)-stranded RNA template. After completion of leader RNA synthesis, the polymerase "jumps" over to the various initiation sites for different mRNA species, probably as a result of "loop out" of the RNA template. The second model proposes that the leader RNA is synthesized and "falls off" the template. This free leader RNA binds to an RNA polymerase, which then initiates mRNA synthesis at various initiation points. The leader RNA serves as a primer for RNA synthesis in this model. The third model proposes that the leader RNA and mRNAs are synthesized independently; after the completion of synthesis, the leader RNA is then joined to the body sequences of the mRNAs post-transcriptionally by an unknown mechanism. Since the data presented in this report suggest that the leader RNA is joined to the mRNAs during de novo synthesis, rather than post-transcriptionally, the third model is not likely. Either the first or the second model could account for the present findings. However, we found that only one RF, which corresponds to the full-length genomic RNA, is produced after RNase A treatment of purified RIs. This suggests that a (−)-stranded RNA is actively synthesizing every viral mRNA and that there are no untranscribed regions (loops) in the RI, as there are during replication of togaviruses (21). This makes the first model, which would have generated subgenomic RFs, less likely. Currently, all available data are compatible with the second model. This model partly resembles the replication of vesicular stomatitis virus, which independently synthesizes a leader RNA (7), and also partly resembles the transcription of influenza virus, which scavenges cellular mRNA cap structures as primers for viral mRNA synthesis (3, 19). If this model for MHV mRNA transcription is correct, a free leader RNA or ribonucleoprotein-associated leader RNA must be present in infected cells and either a leader RNA recognition function is present in the RNA-dependent RNA polymerase or there is sequence complementarity between the leader RNA and six different regions on the (−)-stranded RNA template. Presently, it is not known if either function exists, but experiments are in progress to test these predictions.

MHV RIs have many properties in common with those of poliovirus RIs (1, 23, 28). MHV RIs sediment between 12 and 38S and have an average of 4 to 6.5 nascent strands per RI molecule. However, the calculated number of nascent strands could be misleading since, in contrast to the single mRNA of poliovirus, there are seven genomic and subgenomic MHV mRNAs which are transcribed at the same time, probably on the same RI. Furthermore, these mRNAs are present in widely different abundance (12, 18) and, therefore, presumably are transcribed at different rates and frequencies. This fact could have distorted the calculated number of single-stranded tails. Also, it cannot be excluded that some double-stranded RNA could have been derived from the annealing of the mRNAs with (−)-stranded RNA template during phenol extraction of RNA (26). However, this possibility is less likely, since short-term labeling (15 min) also revealed essentially identical results (data not shown) and oligonucleotide fingerprints of undenatured RIs contained very little poly(A) (Fig. 4A), which would have been present in abundance if the mRNAs randomly annealed to the (−)-stranded template during

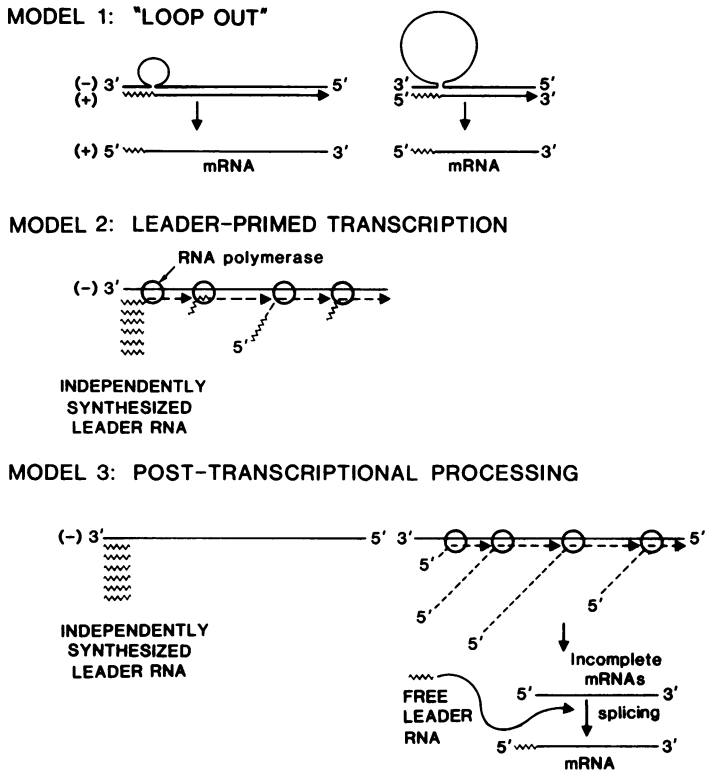

FIG. 6. Possible mechanisms of MHV transcription. Three possible mechanisms are proposed for the joining of leader RNA to the body of each viral mRNA.

phenol extraction. It is not known how the rate of synthesis of different mRNAs is regulated on MHV RIs so that the smallest mRNA becomes the most abundant RNA species (12, 18). It is noteworthy that oligonucleotides 10 and 19 are among the most abundant large T_1 oligonucleotides detected on the fingerprints of RIs. Oligonucleotide 10 represents the sequences within the leader RNA region, whereas oligonucleotide 19 comes from the 5'-terminal regions of mRNAs 7, 3, 2, and 1 (13). However, oligonucleotides, 3a and 19a, which are specific for mRNAs 5 and 6 (12), respectively, could not be detected on the fingerprints of RIs. These observations probably reflect the higher rate of synthesis of mRNA 7, since mRNA 7 is at least 10 times more abundant than any other mRNA (18).

The presence of the cap structure on the nascent chains and the correspondence between the numbers of cap structures and the numbers of nascent chains on MHV RIs provide strong evidence that capping of the mRNAs occurs very rapidly after initiation of the mRNA. This agrees with the observations made in several different animal virus systems (2, 6, 8). MHV RIs, nevertheless, provide the most direct data for this capping mechanism since the functional nascent RNA chains, rather than artificial premature termination products, were examined in this study.

The mRNA synthesis of MHV thus utilized a very unique mechanism for joining the leader RNA to the body sequences of RNA. It has been suggested previously that the late polymerase is responsible for the synthesis of such mRNAs (Brayton et al., submitted for publication). The study of the properties of this RNA-dependent RNA polymerase might shed further light on this unique process.

ACKNOWLEDGMENTS

We thank Mahmood Kafaii for excellent technical assistance and Toni Ferry for editorial assistance in manuscript preparation.

This investigation was supported by Public Health Service grant AI 19244 from the National Institutes of Health, grant RG 1449-A from the National Multiple Sclerosis Society, and grant PCM-4507 from the National Science Foundation. R.S.B. was supported by Public Health Service grant NS 07149 from the National Institutes of Health.

LITERATURE CITED

1. **Baltimore, D.** 1969. The replication of picornaviruses, p. 103–176. *In* H. B. Levy (ed.), The biochemistry of viruses. Marcel Dekker, Inc., New York.
2. **Banerjee, A. K.** 1980. 5'-Terminal cap structure in eucary-

otic messenger ribonucleic acids. Microbiol. Rev. **44**:174–205.
3. **Bouloy, M., S. J. Plotch, and R. M. Krug.** 1978. Globin mRNAs are primers for the transcription of influenza viral RNA in vitro. Proc. Natl. Acad. Sci. U.S.A. **75**:4886–4890.
4. **Brayton, P. R., R. G. Ganges, and S. A. Stohlman.** 1981. Host cell nuclear function and murine hepatitis virus replication. J. Gen. Virol. **56**:457–460.
5. **Brayton, P. R., M. M. C. Lai, C. D. Patton, and S. A. Stohlman.** 1982. Characterization of two RNA polymerase activities induced by mouse hepatitis virus. J. Virol. **42**:847–853.
6. **Chanda, P. K., and A. K. Banerjee.** 1981. Identification of promotor-proximal oligonucleotides and a unique dinucleotide, pppGpC, from in vitro transcription products of vesicular stomatitis virus. J. Virol. **39**:93–103.
7. **Colonno, R. J., and A. K. Bannerjee.** 1976. A unique RNA species involved in initiation of vesicular stomatitis virus RNA transcription in vitro. Cell **8**:197–204.
8. **Darnell, J. E.** 1982. Variety in the level of gene control in eukaryotic cells. Nature (London) **297**:365–371.
9. **Dubin, D. T., V. Stollar, C. C. Hsrchen, K. Timko, and G. M. Guild.** 1977. Sindbis virus messenger RNA: the 5′-termini and methylated residues of 26S and 42S RNA. Virology **77**:457–470.
10. **Jacobs, L., W. J. M. Spaan, M. C. Horzinek, and B. A. M. van der Zeijst.** 1981. Synthesis of subgenomic mRNA's of mouse hepatitis virus is initiated independently: evidence from UV transcription mapping. J. Virol. **39**:401–406.
11. **Lai, M. M. C., P. R. Brayton, R. C. Armen, C. D. Patton, C. Pugh, and S. A. Stohlman.** 1981. Mouse hepatitis virus A59: mRNA structure and genetic localization of the sequence divergence from hepatotrophic strain MHV-3. J. Virol. **39**:823–834.
12. **Lai, M. M. C., C. D. Patton, R. S. Baric, and S. A. Stohlman.** 1983. Presence of leader sequences in the mRNA of mouse hepatitis virus. J. Virol. **46**:1027–1033.
13. **Lai, M. M. C., C. D. Patton, and S. A. Stohlman.** 1982. Further characterization of mRNA's of mouse hepatitis virus: presence of common 5′-end nucleotides. J. Virol. **41**:557–565.
14. **Lai, M. M. C., C. D. Patton, and S. A. Stohlman.** 1982. Replication of mouse hepatitis virus: negative-stranded RNA and replicative form RNA are of genome length. J. Virol. **44**:487–492.
15. **Lai, M. M. C., and S. A. Stohlman.** 1978. RNA of mouse hepatitis virus. J. Virol. **26**:236–242.
16. **Lai, M. M. C., and S. A. Stohlman.** 1981. Comparative analysis of RNA genomes of mouse hepatitis viruses. J. Virol. **38**:661–670.
17. **Laskey, R. A., and A. D. Mills.** 1975. Quantitative film detection of ^{3}H and ^{14}C in polyacrylamide gels by fluorography. Eur. J. Biochem. **56**:335–341.
18. **Leibowitz, J. L., K. C. Wilhemsen, and C. W. Bond.** 1981. The virus specific intracellular species of two murine coronaviruses: MHV-A59 and MHV-JHM. Virology **114**:39–51.
19. **Plotch, S. J., M. Bouloy, I. Ulmanen, and R. M. Krug.** 1981. A unique cap (m^{7}GpppXm)-dependent influenza virion endonuclease cleaves capped RNAs to generate primers that initiate viral RNA transcription. Cell **23**:847–858.
20. **Siddell, S. G., H. Wege, A. Barthel, and V. ter Meulen.** 1981. Coronavirus JHM: intracellular protein synthesis. J. Gen. Virol. **53**:145–155.
21. **Simmons, D. T., and J. H. Straus.** 1972. Replication of Sindbis virus. II. Multiple form of double-stranded RNA isolated from infected cells. J. Mol. Biol. **71**:615–631.
22. **Spaan, W. J. M., P. J. M. Rottier, M. C. Horzinek, and B. A. M. van der Zeijst.** 1982. Sequence relationships between the genome and the intracellular RNA species 1, 3, 6, and 7 of mouse hepatitis virus strain A59. J. Virol. **42**:432–439.
23. **Spector, D. H., and D. Baltimore.** 1975. Polyadenylic acid on poliovirus RNA. II. Poly(A) on intracellular RNAs. J. Virol. **15**:1418–1431.
24. **Sturman, L. S.** 1977. Characterization of a coronavirus. I. Structural proteins: effects of preparative conditions on the migration of protein in polyacrylamide gels. Virology **77**:637–649.
25. **Wege, H., A. Miller, and V. ter Meulen.** 1978. Genomic RNA of the murine coronavirus JHM. J. Gen. Virol. **41**:217–227.
26. **Weissmann, C., G. Feix, and H. Slor.** 1968. *In vitro* synthesis of phage RNA: the nature of the intermediates. Cold Spring Harbor Symp. Quant. Biol. **33**:83–100.
27. **Wilhelmsen, K. C., J. L. Leibowitz, C. W. Bond, and J. A. Robb.** 1981. The replication of murine coronaviruses in enucleated cells. Virology **110**:225–230.
28. **Yogo, Y., and E. Wimmer.** 1975. Sequence studies of poliovirus RNA. III. Polyuridylic acid and polyadenylic acid as components of the purified poliovirus replicative intermediate. J. Mol. Biol. **92**:467–477.